Resonant states of ${}^{9}_{\Lambda}$Be with $\alpha + \alpha + \Lambda$ three-body cluster model

Qian Wu [1,*] Yasuro Funaki [2,3,†] Emiko Hiyama [4,3,‡] and Hongshi Zong [1,5,6,7,§]

[1] *Department of Physics, Nanjing University, Nanjing 210093, China*
[2] *College of Science and Engineering, Kanto Gakuin University, Yokohama 236-8501, Japan*
[3] *RIKEN Nishina Center, RIKEN, 2-1 Hirosawa, 351-0115 Saitama, Japan*
[4] *Department of Physics, Kyushu University, 819-0395, Fukuoka, Japan*
[5] *Nanjing Proton Source Research and Design Center, Nanjing 210093, China*
[6] *Department of Physics, Anhui Normal University, Wuhu, Anhui 241000, China*
[7] *Joint Center for Particle, Nuclear Physics and Cosmology, Nanjing 210093, China*

(Received 4 December 2019; accepted 14 October 2020; published 2 November 2020)

We study the structure of ${}^{9}_{\Lambda}$Be within the framework of the three-body $\alpha + \alpha + \Lambda$ cluster model using the YNG-NF interaction with the Gaussian expansion method. We obtain the energies of bound states as well as energies and decay widths of the resonant states with the complex scaling method. By analyzing our wave functions of bound states and resonant states, we confirm three analog states of ${}^{9}_{\Lambda}$Be pointed out by Bandō and Motoba *et al.* [T. Motoba, H. Bandō, and K. Ikeda, Prog. Theor. Phys. **70**, 189 (1983); T. Motoba, H. Bandō, K. Ikeda, and T. Yamada, Prog. Theor. Phys. Suppl. **81**, 42 (1985); H. Bandō, K. Ikeda, and T. Motoba, Prog. Theor. Phys. **69**, 918 (1983)], ^{8}Be analog states, ${}^{9}_{\Lambda}$Be genuine states, and ^{9}Be analog states. The new states of ${}^{9}_{\Lambda}$Be are also obtained at a high energy region with broader decay widths.

DOI: 10.1103/PhysRevC.102.054303

I. INTRODUCTION

One of the main goals in hypernuclear physics is to explore the new dynamical feature by an addition of a Λ particle. Since there is no effect of the Pauli principle between nucleons and a Λ particle, participation of Λ particle in nuclei gives rise to more bound states. As a result, a significant contraction of nuclear cores is caused. We call this phenomena as 'glue-like' role of a Λ particle. Such a study for the energy stability in light hypernuclei has been investigated in Refs. [1–5] for stable nucleus plus a Λ particle, and for neutron-rich nuclei plus a Λ particle [6].

One of the typical examples is a combination of ^{6}He and ${}^{7}_{\Lambda}$He. The core nucleus ^{6}He is known to be a halo nucleus whose observed binding energy of the ground state is -0.96 MeV, weakly binding with respect to the $\alpha + n + n$ breakup threshold. In Ref. [6], it is predicted that the ground state of ${}^{7}_{\Lambda}$He should become more bound due to the glue-like role of a Λ particle and that the calculated Λ-separation energy, B_{Λ} was 5.44 MeV within the framework of the ${}^{5}_{\Lambda}\mathrm{He} + N + N$ three-body model. (Afterwards, within the framework of the $\alpha + \Lambda + N + N$ four-body model, it was predicted that $B_{\Lambda} = 5.36$ MeV [7].) In 2013, this neutron-rich Λ hypernucleus was observed for the first time at JLab by a ${}^{7}\mathrm{Li}(e, e'K^{+}){}^{7}_{\Lambda}\mathrm{He}$ reaction and it was reported that $B_{\Lambda} = 5.58 \pm 0.03$ MeV [8], i.e., the energy gain of 5.58 MeV, due to the participation of the Λ particle.

Also, dynamical contraction by the addition of a Λ particle has been studied by many authors [1–3,6,9–12]. Historically, in Refs. [1,2], they studied light p-shell Λ hypernuclei such as ${}^{7}_{\Lambda}$Li, ${}^{8}_{\Lambda}$Li, ${}^{8}_{\Lambda}$Be, and ${}^{9}_{\Lambda}$Be with the microscopic $\alpha + x + \Lambda$ three-body cluster model ($x = d, t, {}^{3}\mathrm{He}$) together with the $\alpha + x$ two-body cluster model for the nuclear core. They pointed out that reduction of the $B(E2)$ strength led to the contraction of the hypernuclear size since the $B(E2)$ was proportional to the fourth power of the distance between the α and x clusters and then they predicted that the α-x distances in $A = 7$–9 Λ hypernuclei should be reduced by about 20%. Afterwards, in Ref. [6], the experimentalists were proposed to measure $B(E2)$ of $5/2^{+} \rightarrow 1/2^{+}$ in ${}^{7}_{\Lambda}$Li and predicted $B(E2) = 2.42\, e^{2}\mathrm{fm}^{4}$ with the ${}^{5}_{\Lambda}\mathrm{He} + N + N$ three-body cluster model. At KEK, the measurement of this hypernucleus was done successfully and they reported $B(E2) = 3.6 \pm 0.5\, e^{2}\mathrm{fm}^{4}$, where the shrinkage effect was confirmed by an addition of the Λ particle [13].

Another interesting issue in hypernuclear physics is to find new states due to the injection of Λ particle. For this study, Bandō and Motoba *et al.* [1–3] investigated the level structure of ${}^{9}_{\Lambda}$Be within an $\alpha + \alpha + \Lambda$ three-body model and categorized three types of states, '^{8}Be analog states', '^{9}Be analog states', and '${}^{9}_{\Lambda}$Be genuine states', according to the SU(3) shell model classification. The ^{8}Be analog state corresponds to the SU(3) irreducible representation with $[s^{5}p^{4}](\lambda, \mu) = (4, 0)$, where the Λ particle occupies the $(0s)$ orbit. Bandō and Motoba *et al.* defined two ${}^{8}\mathrm{Be} + \Lambda(0p)$ configurations as '^{9}Be analog states' and '${}^{9}_{\Lambda}$Be genuine states', corresponding to the

*wuqian@smail.nju.edu.cn
†yasuro@kanto-gakuin.ac.jp
‡hiyama@riken.jp
§zonghs@nju.edu.cn

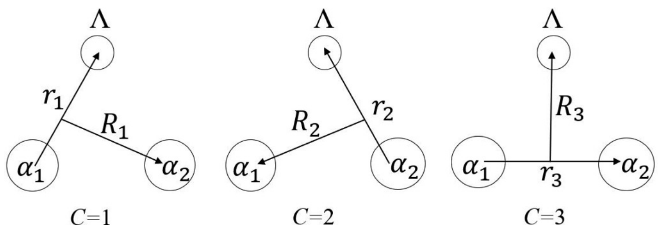

FIG. 1. Jacobian coordinates of ${}^{9}_{\Lambda}$Be with the $\alpha + \alpha + \Lambda$ model.

$[s^4p^5](\lambda,\mu) = (3, 1)$ and $[s^4p^5](\lambda\mu) = (5, 0)$ irreducible representations, respectively. The latter is a new symmetry called 'supersymmetric' by Dalitz and Gal [14,15]. In view of weak coupling, or of nuclear clustering, in these configurations the Λ particle is supposed to orbit around a well developed α-α core since the ^{8}Be core has a well developed 2α cluster structure. In particular, in the ^{9}Be-analog states and ${}^{9}_{\Lambda}$Be genuine states, the Λ particle occupies two kinds of p orbit, which are perpendicular and parallel to the deformation axis of the α-α core, respectively.

Here, it should be noted that Bandō and Motoba *et al.* [1–3] obtained three categorized states, almost all states of which are resonant states above the lowest threshold ${}^{5}_{\Lambda}\mathrm{He} + \alpha$ obtained by using the bound state approximation with restricted configuration, where they took only one Jacobian coordinate of $(\alpha\alpha) - \Lambda$ channel (see of $C = 3$ in Fig. 1) using a small number of basis functions for α-α ($\boldsymbol{r}_3$ of Fig. 1) and $(\alpha\alpha) - \Lambda$ ($\boldsymbol{R}_3$ of Fig. 1) coordinates. It is considered that the bound state approximation works for sharp resonant states, but it would be difficult to obtain broader resonant states.

To obtain resonant states theoretically, there have been many achievements (for instance, see Ref. [16]). One of the successful methods is the complex scaling method (CSM) [17–21].

For this purpose, recently, using CSM and the Gaussian expansion method (GEM), we obtained all of the possible resonant states of ${}^{9}_{\Lambda}$Be within the framework of the $\alpha + \alpha + \Lambda$ three-body model [22]. In Ref. [22], we found that energies and ordering of some resonant states were consistent with those by Motoba *et al.*, and some were different from the results of Bandō and Motoba *et al.* [1–3]. However, we have not analyzed the category of these states proposed in Ref. [22] in detail.

Therefore, in this work, we calculate the energy spectra of bound states as well as of resonant states with the $\alpha + \alpha + \Lambda$ three-body model + CSM using the same $\alpha\Lambda$ interaction as used in Ref. [22]. By comparing our wave functions with those of the SU(3) shell-model wave functions, we confirm that the ^{8}Be analog states, ^{9}Be analog states, and ${}^{9}_{\Lambda}$Be genuine states appear, as discussed by Bandō and Motoba *et al.* [1–3]. We also find new states at around 10–20 MeV above the $\alpha + \alpha + \Lambda$ three-body breakup threshold, which have never been pointed out by Bandō and Motoba *et al.*

Finally, we discuss our calculated states in comparison with observed data [23,24].

This paper is organized as follows. In Sec. II, we introduce the realistic NN and ΛN interaction and the unique adjustments of the some parameters. After explaining the method employed, we show the results and the discussion of ${}^{9}_{\Lambda}$Be. Summary is given in Sec. IV.

II. METHOD AND HAMILTONIAN

Since we investigate the ${}^{9}_{\Lambda}$Be within the framework of the $\alpha + \alpha + \Lambda$ three-body cluster model, the Hamiltonian is then defined as

$$H = T + V_{\alpha_1\alpha_2} + \sum_{i=1}^{2} V_{\alpha_i\Lambda} + V^{\mathrm{Pauli}}_{\alpha_1\alpha_2}, \tag{1}$$

where T is the kinetic energy operator. $V_{\alpha_1\alpha_2}$ and $V_{\alpha\Lambda}$ represent the α-α interaction and α-Λ interaction, respectively. The $V^{\mathrm{Pauli}}_{\alpha_1\alpha_2}$ stands for the Pauli exclusion operator acting between 2αs, explained below.

In order to solve the Schrödinger equation, the Gaussian Expansion method [25,26] enables us to use three sets of Jacobian coordinates ($C = 1$–3) of Fig. 1 in our total trial wave function:

$$\Psi_{JM} = \sum_{c=1}^{3}\sum_{I}\sum_{\ell,L}\sum_{n,N} C^{(c)}_{n\ell NLI}\mathscr{S}_\alpha\big\{\big[\phi_{\alpha_1}\phi_{\alpha_2}\big] \times\big[\phi^{(c)}_{n\ell}(\mathbf{r}_c)\psi^{(c)}_{NL}(\mathbf{R}_c)\big]_I\chi_{\frac{1}{2}}(\Lambda)\big\}_{JM}, \tag{2}$$

where $\mathscr{S}_\alpha$ is the α-α symmetrization operator and ϕ_{α_i} is the intrinsic wave function of α with $(0s)^4$ configuration. $\chi_{\frac{1}{2}}(\Lambda)$ is the spin function of Λ. Since the energy splitting of $3/2^+ - 5/2^+$ is almost negligible measured by the high-resolution γ-ray experiment [27,28], we neglect the spin-orbit force between α and Λ and simply regard I as J. And the spatial part $\phi_{n\ell m}(\mathbf{r})$ and $\psi_{NLM}(\mathbf{R})$ have the form

$$\phi_{n\ell m}(\mathbf{r}) = r^{\ell}e^{-(r/r_n)^2}Y_{\ell m}(\hat{\mathbf{r}}),$$
$$\psi_{NLM}(\mathbf{R}) = R^{L}e^{-(R/R_N)^2}Y_{LM}(\hat{\mathbf{R}}), \tag{3}$$

where the Gaussian variational parameters are chosen to have geometric progression:

$$r_n = r_{\min}a^{n-1}, \quad (n = 1 \sim n_{\max}),$$
$$R_N = R_{\min}A^{N-1}, \quad (N = 1 \sim N_{\max}). \tag{4}$$

Both the eigenenergies and the coefficients C are obtained by using the Rayleigh-Ritz variational method. In our calculation, we adopt $l(L)$ to be up to 4 and $n(N)$ to be up to 15. The $\Lambda\alpha$ interaction is obtained by folding the ΛN interaction into the α cluster wave function. We use a so-called YNG interaction which simulated G-matrix ΛN interaction derived from Nijmegen model $f(NF)$ by the three-range Gaussian form as a function of k_F. The YNG interaction is given as

$$V_{\Lambda N}(r,k_F) = \sum_{i=1}^{3}\Bigg[\Big(v^i_{0,\mathrm{even}} + v^i_{\sigma\sigma,\mathrm{even}}\sigma_\Lambda\sigma_N\Big)\frac{1+P_r}{2} +\big(v^i_{0,\mathrm{odd}} + v^i_{\sigma\sigma,\mathrm{odd}}\sigma_\Lambda\sigma_N\big)\frac{1-P_r}{2}\Bigg]e^{-(r/\beta_i)^2}, \tag{5}$$

where P_r is the space exchange operator. The strengths $v^i_{0,\mathrm{even}}$, $v^i_{\sigma\sigma,\mathrm{even}}$, $v^i_{0,\mathrm{odd}}$, and $v^i_{\sigma\sigma,\mathrm{odd}}$ are represented as functions of k_F

TABLE I. ΛN interaction depth $v^{i}_{0,\text{even}}$ and $v^{i}_{0,\text{odd}}$ of the modified *YNG-NF* model. Here, we take $k_F = 0.963$ fm^{-1}.

β_i(fm)	1.50	0.90	0.50
$v^{i}_{0,\text{even}}$	-9.22	-187.63	795.43
$v^{i}_{0,\text{odd}}$	-5.67	-35.26	2141.79

in Eq. (2.7) of Ref. [29]. The parameters of the *NF* model are fixed to reproduce the observed binding energy of ${}^{5}_{\Lambda}$He. However, it is pointed out that the *NF* model causes an overbound problem for the ground state of ${}^{9}_{\Lambda}$Be, due to the strong attraction of odd-state component of spin independent part of the ΛN interaction [26]. In this case, we tune the odd state part and k_F to reproduce the observed binding energy of ${}^{5}_{\Lambda}$He and ${}^{9}_{\Lambda}$Be. The new parameters of the modified *NF* model are listed in Table I.

The Pauli principle between two α clusters is taken into account with the orthogonality condition model (OCM). The OCM projection operator is represented by

$$V^{\text{Pauli}}_{\alpha_1\alpha_2} = \lim_{\lambda\to\infty} \lambda \sum_{f=0s,1s,0d} \left|\phi_f(\mathbf{r}_{\alpha_1\alpha_2})\right\rangle\left\langle\phi_f(\mathbf{r}'_{\alpha_1\alpha_2})\right|. \quad (6)$$

The Pauli forbidden states $(0s, 1s, 0d)$ are ruled out when λ is an infinity number and practically the λ is given around $\approx 10^5$ MeV, which is high enough to push the unphysical states into a large energy region without affecting the physical states.

We use the α-α interaction, which reproduces the observed α-α scattering phase shift and the ground state of ^{8}Be with the α-α OCM. In this case, we fold the modified Hasegawa-Nagata effective *NN* potential and *pp* Coulomb potential into the α cluster wave function.

In this work, we calculate both the bound state and resonant state with the use of the CSM [17–21], which enables us to obtain the energy and decay width of the resonant state. The CSM is considered to be almost a unique method to deal with many-body resonances, more than two-body systems [30–33]. By solving the complex scaled Schrödinger equation with a scaling angle θ:

$$[H(\theta) - E(\theta)]\ \Psi(\theta) = 0, \quad (7)$$

where the scaling Hamiltonian is obtained by setting

$$r_c \to r_c e^{i\theta}, \quad R_c \to R_c e^{i\theta}, \quad (8)$$

the energy eigenvalue is obtained, independently of θ, as a complex number, $E = E_r - i\Gamma/2$, where the width and energy of the resonance are E_r and Γ, respectively. The bound state will be stable in the negative real axis while the continuum states are rotated downwards at an angle of 2θ with the real axis. In Fig. 2, we present two typical examples in calculating the resonant states of ${}^{9}_{\Lambda}$Be using the CSM. In these two figures, the resonance remains stable when θ increases and the poles become isolated from the continuum states. Moreover, we can see three series of lines for continuum states in Fig. 2, corresponding to the ${}^{5}_{\Lambda}$He$(0^+)+\alpha$ threshold, the $\alpha + \alpha + \Lambda$ and ^{8}Be$(0^+)+\Lambda$ thresholds, both of which are not distinguished in these figures, and the ^{8}Be$(2^+)+\Lambda$ threshold.

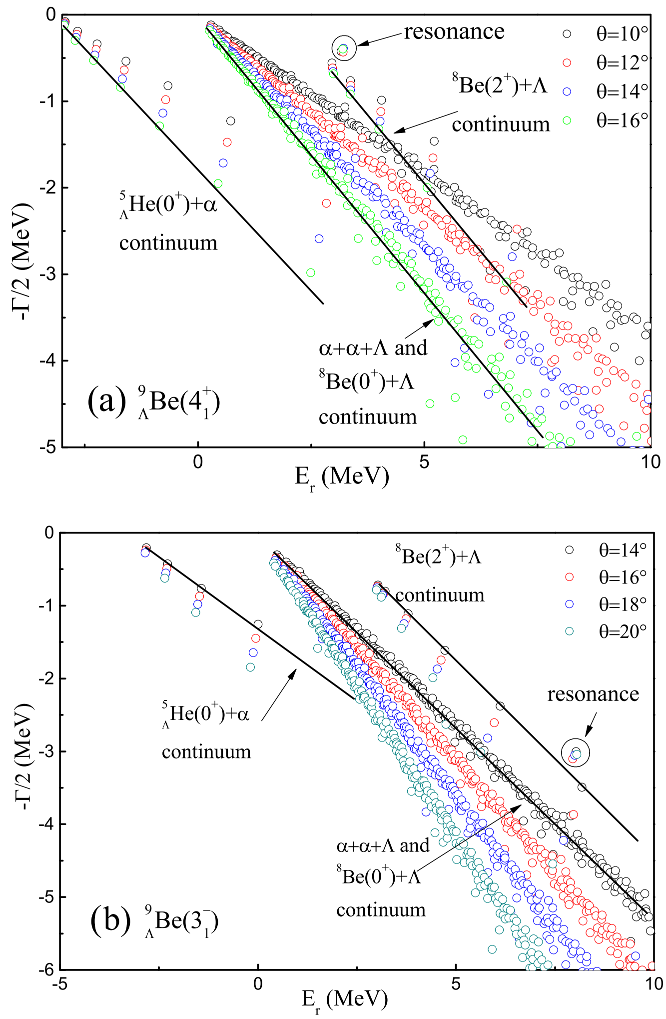

FIG. 2. Dependence of the energy distribution on the complex scaling angle θ for ${}^{9}_{\Lambda}$Be. Two different cases are considered: (a) presence of a narrow resonance with $J^{\pi} = 4^+$ at $E_r = 3.2$ MeV with $\Gamma = 0.78$ MeV and (b) presence of a broad resonance with $J^{\pi} = 3^-$ at $E_r = 9.4$ MeV with $\Gamma = 7.1$ MeV

III. RESULTS AND DISCUSSION

A. Energy spectra of ${}^{9}_{\Lambda}$Be

We show the energy spectra of ${}^{9}_{\Lambda}$Be obtained by the OCM + CSM in a)–d) of Fig. 3. We also show at the leftmost column the 0^+_1, 2^+_1, and 4^+_1 resonant states of ^{8}Be, which are obtained by the same framework. For later convenience, we group them into a), b), c), and d). In all of the subsequent calculations, the spin-orbit splitting of the Λ particle and core is neglected since it is very small.

First, we discuss the spectra of positive parity states of ${}^{9}_{\Lambda}$Be, 0^+_1, 2^+_1, and 4^+_1 states [a) of Fig. 3]. As we can see, the 0^+_1 and 2^+_1 states are the bound by 3.82 MeV and 6.65 MeV, respectively, with respect to the $\alpha + \alpha + \Lambda$ threshold. Thus, the calculated B_Λ for the ground state is equal to 6.74 MeV and it is noted that we adjust the odd state of *YNG-NF* interaction so as to reproduce the experimental data, $B_\Lambda = 6.71 \pm 0.04$ MeV [34]. The excitation energy for the 2^+_1 state,

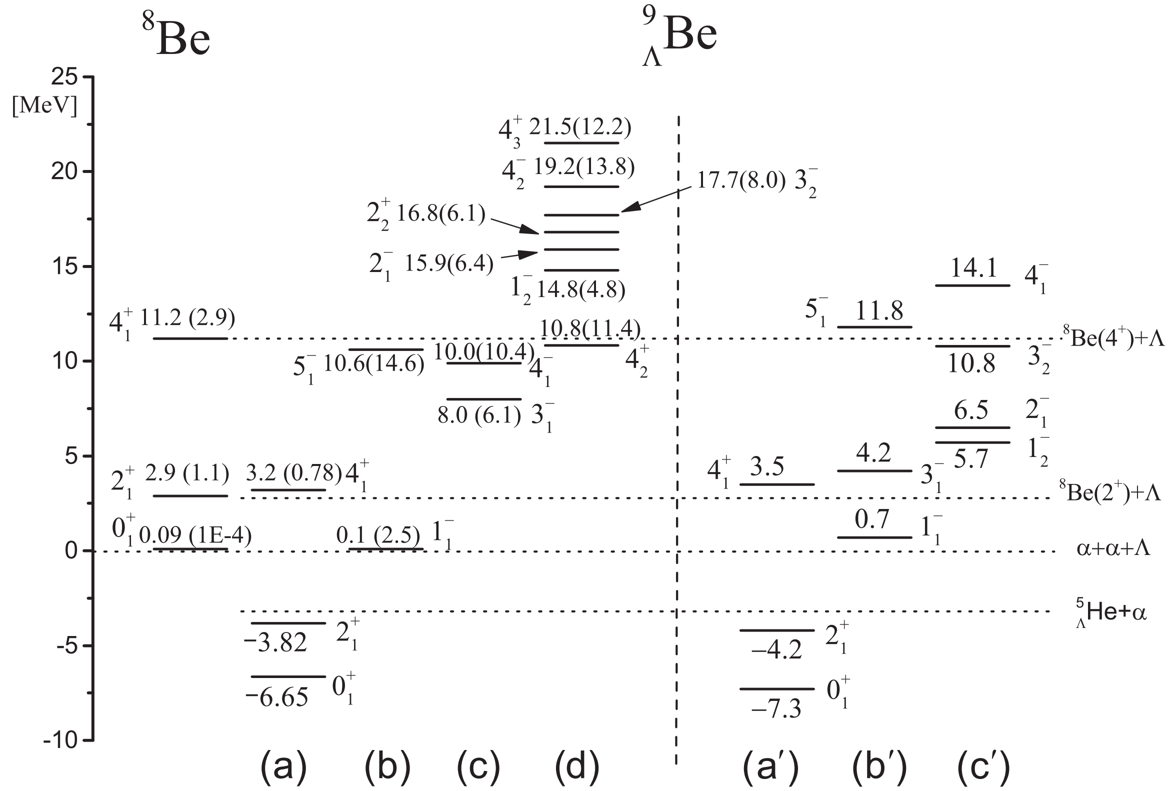

FIG. 3. Calculated energy spectra of ^{8}Be and $^9_\Lambda$Be with respect to $\alpha+\alpha+\Lambda$ three-body threshold. The values in parenthesis are decay widths. The spectra are categorized as a) ^{8}Be analog band, b) $^9_\Lambda$Be genuine states, c) ^{9}Be analog states and d) new states. And the calculate energy spectra of $^9_\Lambda$Be by Motoba *et al.* [2] are located in columns a′), b′), and c′): a′) ^{8}Be analog band, b′) $^9_\Lambda$Be genuine states, c′) ^{9}Be analog states.

$E_{\rm ex} = 2.83$ MeV, is in good agreement with the observed value, $E_{\rm ex} = 3.079 \pm 0.040$ MeV [35]. The 4^+_1 state is obtained as a resonance, whose energy and width are calculated to be $E_r = 3.2$ MeV, above the $\alpha+\alpha+\Lambda$ threshold with $\Gamma = 0.78$ MeV, respectively. In Refs. [1–3], the authors pointed out that these states are ^{8}Be analog states, in which the Λ particle couples in an s wave to the 0^+_1, 2^+_1, and 4^+_1 states of ^{8}Be.

Next, we discuss the resonant states with CSM. Here, we rotate θ to be up to 26 degrees which is the limitation of our calculation. In column b) of Fig. 3, we show two resonant states, 1^-_1 and 5^-_1 states at $E_r = 0.1$ MeV with $\Gamma = 2.5$ MeV and $E_r = 10.6$ MeV with $\Gamma = 14.6$ MeV, respectively. These states may correspond to the so-called $^9_\Lambda$Be genuine hypernuclear states pointed out in Refs. [1–3], in which the Λ particle occupies a p orbit in a parallel direction to the $\alpha+\alpha$ axis of the ^{8}Be core. This Λ particle motion is made possible because of no active effect of the Pauli principle of the Λ particle to nucleons in the ^{8}Be core, unlike the case of ^{9}Be.

In column c) of Fig. 3, we obtain the 3^-_1 and 4^-_1 resonant states at $E_r = 8.0$ MeV with $\Gamma = 6.1$ MeV and $E_r = 10.0$ MeV with $\Gamma = 10.4$ MeV, which can be categorized as '^{9}Be analog states'. This means that in these states the Λ particle occupies a p orbit around the ^{8}Be core, which is perpendicular to the α-α axis, like a neutron orbiting around ^{8}Be core in ^{9}Be nucleus.

In column d) of Fig. 3, we show several resonant states such as 4^+_2, 1^-_2, 2^-_1, 2^+_2, 3^-_2, 4^-_2, and 4^+_3, which are located at much higher energy regions above the $\alpha+\alpha+\Lambda$ threshold. These states are not obtained in Refs. [1–3] and more details will be discussed later in Sec. III C.

For comparison, in columns a′), b′), and c′) of Fig. 3, we show the energy spectra of $^9_\Lambda$Be obtained by Motoba *et al.* [2], in which the *YNG-NF* potential for the Λ-nucleon interaction is adopted. Here, we can see that their binding energy of the ground state is overbound compared with the observed data. This overbinding behavior is caused by a strong attraction of the odd-state part of the *YNG-NF* potential, as mentioned in Sec. II (see also Ref. [26]). We should note that their calculations are performed within the bound state approximation, in spite of the fact that almost all states shown here are located in an unbound region, with a finite decay width.

As pointed out by Bandō and Motoba *et al.* [1–3], the energy spectra of $^9_\Lambda$Be are categorized in ^{8}Be analog states, $^9_\Lambda$Be genuine states, and ^{9}Be analog states, which are shown in columns a′), b′), and c′) of Fig. 3, respectively. In column a′), their binding energies of 0^+, 2^+, and 4^+ states are similar to ours. As for the $^9_\Lambda$Be genuine states in column b′) of Fig. 3, their energies of the 1^-_1 and 5^-_1 states are very close to the 1^-_1 and 5^-_1 states in our calculation shown in column b). We have to emphasize that in our calculation, we have no 3^-_1 state corresponding to the 3^- state in $^9_\Lambda$Be genuine states in column b′) of Fig. 3. In column c′) of Fig. 3, which can be categorized as the ^{9}Be analog states, the binding energies of the 3^-_2 and

4_1^- states are slightly higher than those of our 3_1^- and 4_1^- states shown in column c).

On the other hand, we cannot find any 1^- and 2^- resonant states in the energy region of the 1_2^- and 2_1^- states shown in column c′) of Fig. 3. The discrepancy of the energy spectra obtained by the resonance treatment like the present CSM and by the bound state approximation will be discussed in detail in the next subsection.

B. ^{8}Be analog, ^{9}Be analog, and ${}^9_\Lambda$Be genuine states

In this subsection, we discuss the structure of the states in columns a), b), and c) of Fig. 3, and also discuss the reason why our spectra in columns b) and c) do not have one-to-one correspondence to those obtained by Bandō and Motoba *et al.* in Refs. [1–3].

First, we find that the 0_1^+, 2_1^+, and 4_1^+ states in column a) have the analogous structure to the 0_1^+, 2_1^+, and 4_1^+ states of ^{8}Be, respectively, as is consistent with the results in Refs. [1–3]. In fact, for these three states we calculate the s-wave components of the Λ particle coupling to the ^{8}Be core, which are found to be very large, 96%, 95%, and 93%, for the 0_1^+, 2_1^+, and 4_1^+ states, respectively. This is nothing but the ^{8}Be analog structure, where the configurations ${}^8\mathrm{Be}(0^+)+\Lambda$, ${}^8\mathrm{Be}(2^+)+\Lambda$, and ${}^8\mathrm{Be}(4^+)+\Lambda$, are realized for the 0_1^+, 2_1^+, and 4_1^+ states, respectively. Bandō and Motoba *et al.* also obtained in Refs. [1–3] the similar values, around 95%, for these states, and hence we can say that our spectra in column a) reproduce those states in column a′) in Fig. 3 obtained in Refs. [1–3].

As explained in Sec. I, the classification of the spectra shown in columns a′)–c′) in Fig. 3 is, in a strong coupling limit, better understood by the nuclear SU(3) model, where the columns a′), b′), and c′) correspond to the SU(3) irreducible representations, $(\lambda,\mu)=(4,0)$, (5,0), and (3,1), respectively. In order to investigate how much our spectra also keep this strong coupling SU(3)-like nature, we compare our wave functions with the corresponding relative wave functions between the two-α clusters and Λ particle described in terms of the SU(3) shell model picture.

From this aspect, we next discuss the 1_1^- state in column b) of Fig. 3. However, since this state is obtained by the CSM, as having a very broad width, it is no more trivial to physically interpret any physical quantities calculated by using the resonant wave function. Thus we first construct an approximate 1_1^- wave function in a bound state region, so as to be smoothly connected to the resonant 1_1^- wave function with the broad width. That can be done by introducing the following attractive three-body force and artificially changing the resonant wave function to a bound state wave function, to analyze the wave function without any difficulty:

$$V=V_0e^{-\mu(r_1^2+r_2^2+r_3^2)},\tag{9}$$

where μ is fixed to be 0.1 fm^{-2}. When we choose $V_0=-110$ MeV, the 1_1^- state becomes a weakly bound state, whose binding energy is 0.28 MeV relative to the ${}^5_\Lambda\mathrm{He}+\alpha$ threshold. We hereafter denote this artificial 1^- state as the 1_I^- state.

On the other hand, according to the Bayman-Bohr theorem [37], the SU(3) $(\lambda,\mu)=(5,0)$ and $(\lambda,\mu)=(3,1)$ irreducible representations can be expressed below, in terms of the α cluster wave function

$$|(0s)^4(0p)^4(0p)^1_\Lambda(5,0)J=1\rangle_{\text{internal}}\propto\sum_{l=0,2}C_l^{(5,0)}\mathscr{A}\big|(4l,11)_{J=1}\phi_{\alpha_1}\phi_{\alpha_2}\big\rangle,\tag{10}$$

$$|(0s)^4(0p)^4(0p)^1_\Lambda(3,1)J=1\rangle_{\text{internal}}\propto\sum_{l=0,2}C_l^{(3,1)}\mathscr{A}\big|(4l,11)_{J=1}\phi_{\alpha_1}\phi_{\alpha_2}\big\rangle,\tag{11}$$

where $C_l^{(\lambda,\mu)}=\langle(4,0)_l(1,0)_1||(\lambda,\mu)_1\rangle$, which are the reduced Clebsch-Gordan coefficients of the SU(3) group for the vector coupling $(4,0)\otimes(1,0)=(5,0)\oplus(3,1)$ with $C_{l=0}^{(5,0)}=C_{l=2}^{(3,1)}=\sqrt{7/15}$ and $C_{l=2}^{(5,0)}=-C_{l=0}^{(3,1)}=\sqrt{8/15}$. We use the same coefficients as Eq. (3.4) in Ref. [3] which may be different from the standard SU(3) phase convention [38,39]. $\mathscr{A}$ is the antisymmetrization operator acting on the nucleons, ϕ_{α_i} is the intrinsic wave function of the α particle, and $(nl,NL)_J$ is the harmonic oscillator wave functions for the relative motions between the two-α and Λ particles defined below:

$$|(nl,NL)_J\rangle=[R_{nl}(\boldsymbol{r}_3),R_{NL}(\boldsymbol{R}_3)]_J\rangle.\tag{12}$$

Here, the $\boldsymbol{r}_3(\boldsymbol{R}_3)$ are the Jacobian coordinate set of $C=3$ channel defined in Fig. 1. We then define a normalized relative wave function between the α clusters and Λ particle, corresponding to the SU(3) irreducible representations

$$|(5,0)_1\rangle\equiv\sum_{l=0,2}C_l^{(5,0)}|(4l,11)_{J=1}\rangle,$$
$$|(3,1)_1\rangle\equiv\sum_{l=0,2}C_l^{(3,1)}|(4l,11)_{J=1}\rangle,\tag{13}$$

and calculate the squared overlap between our 1_I^- state and the relative wave functions defined above, i.e., $|\langle(\lambda,\mu)_1|1_I^-\rangle|^2$. We obtain 0.45 and 0.01 for the $(5,0)_1$ and $(3,1)_1$ states, respectively, indicating that our 1_I^- state is much closer to the $(5,0)_1$ state than to the $(3,1)_1$ state (see Table II).

TABLE II. Squared overlap of the ‘artificial’ 1_I^- and 1_{II}^- states with the relative wave functions of the SU(3) shell model defined in Eq. (13). See text for the definition of the ‘artificial’ 1_I^- and 1_{II}^- states.

1_λ^-	$(5,0)_1$	$(3,1)_1$
1_I^-	0.45	0.01
1_{II}^-	$0.01+0.001i$	$0.39+0.02i$

The reason why we obtain at most around 0.5 for the squared overlap with the SU(3)-like configuration can be understood by comparing the SU(3) $(\lambda,\mu)=(4,0)$ irreducible representation and our 0_1^+, 2_1^+, and 4_1^+ wave functions. In the same way as the $(\lambda,\mu)=(3,1)$, (5,0) cases, the SU(3) irreducible representation corresponding to the ^{8}Be analog states, $(\lambda,\mu)=(4,0)$ can be given below, in terms of the α cluster wave function,

$$\big|(0s)^4(0s)^1_\Lambda(0p)^4(4,0)J\big\rangle_{\text{internal}}\propto\mathscr{A}|(4J,00)_J\phi_\alpha\phi_\alpha\rangle.\tag{14}$$

TABLE III. Squared overlaps with the harmonic oscillator relative wave functions, of 0_1^+, 2_1^+, and 4_1^+.

J_1^+	$\lvert\langle(4J,00)_J\lvert J_1^+\rangle\rvert^2$
0_1^+	37%
2_1^+	37%
4_1^+	39%

We then calculate the squared overlap between our wave functions for the 0_1^+, 2_1^+, and 4_1^+ states and the harmonic oscillator wave functions for the relative motions between the α clusters and Λ particle, $|\langle(4J,00)_J|J_1^+\rangle|^2$. We show in Table III the squared overlap values, which are about 40% for all the 0_1^+, 2_1^+, and 4_1^+ states. Since in these states the Λ particle couples to the ^{8}Be core in an s wave with almost 100%, these rather small values indicate that the relative motion between the two-α clusters is excited strongly from the lowest $4\hbar\omega$ harmonic oscillator state, and the α clusters are loosely coupled to each other.

Thus the squared overlap value 0.45 is comparable to the values, around 0.40, for the 0_1^+, 2_1^+, and 4_1^+ states shown in Table III. We can therefore say that asymptotically the 1_1^- state has considerable components of the $^9_\Lambda$Be genuine hypernuclear structure and corresponds to the 1_1^- state in column b′) in Fig. 3.

Next let us compare in more detail our spectra with those obtained in Ref. [2], shown in columns a′)–c′) of Fig. 3. As mentioned in the previous section, we notice that in our spectra the 3^- state in column b), the 1^- and 2^- states in column c) are missing, to have one-to-one corresponding relations with the spectra in columns b′) and c′). One possibility is that these ‘missing’ states exist but we cannot find them because of the limitation of the rotating angle θ in CSM, which is around 26 degrees as we mentioned in the previous subsection. If so, the decay widths of these ‘missing’ states should be much broader than what is estimated in Ref. [2]. It should, however, be noted that the spectra in Ref. [2] are obtained with the bound state approximation, while ours are obtained by taking into account the correct boundary condition of resonances. Then in order to understand how this discrepancy comes out, we try to investigate how the energy poles of the missing resonances disappear in the framework of CSM.

We first solve the present three-body problem in a restricted model space, where only $C=1$ and $C=2$ channels in Fig. 1, i.e., the $^5_\Lambda$He $+\alpha$ channel, are taken into account, to apply the CSM. The complex energies of $J^\pi=3^-$ states for several rotation angles θ are shown in Fig. 4. We can clearly see an energy pole at $E_r=3.6$ MeV with $\Gamma=3.0$ MeV, which is similar to the energy of the 3_1^- state in column b′) of Fig. 3. However, once we incorporate the $C=3$ channel configurations in our three-body model space, the energy pole cannot be distinguished any more from the continuum states, and disappears. Since the inclusion of configurations of channel $C=3$ makes it easier to incorporate ^{8}Be - Λ configurations, it is considered that the “missing” 3^- state is dominated by a large amount of continuum components in the ^{8}Be $+\Lambda$ channel, and it can no longer survive as a resonance with a reasonable width.

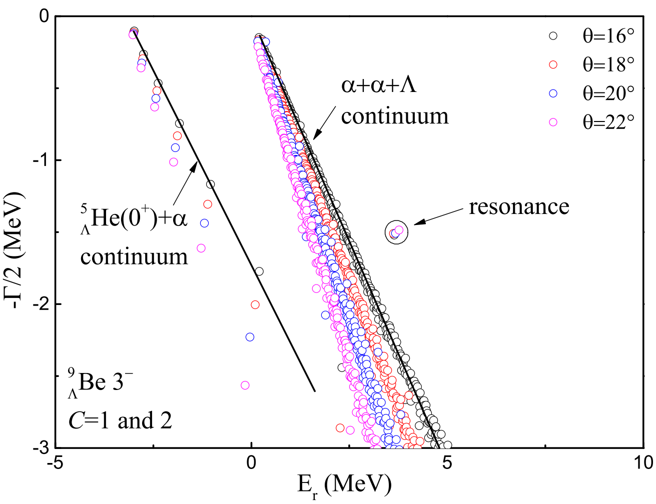

FIG. 4. Dependence of the energy distribution on the complex scaling angle θ for $^9_\Lambda$Be in the case of $C=1$ only. The 3^- state shows up at $E_r=3.6$ MeV with $\Gamma=3.0$ MeV.

In the same way as the 3^- state, we also calculated 1^- and 2^- states in the restricted configurations with $C=1$ and $C=2$ channels only, to apply the CSM. Then we found one sharp resonant state for $J^\pi=1^-$ at $E_r=4.6$ MeV with $\Gamma=2.6$ MeV and also one sharp resonant state for $J^\pi=2^-$ at $E_r=5.6$ MeV with $\Gamma=2.9$ MeV. [See the blue color levels of 1^- and 2^- in column c) of Fig. 5].

In order to clarify the difference of the 1^- state obtained in this way from the 1_1^- state obtained at $E_r=0.1$ MeV, or to elucidate the SU(3)-like nature of this 1^- state, we calculate the squared overlap with the harmonic oscillator wave functions, defined by Eq. (13), corresponding to the SU(3) $(\lambda,\mu)=(3,1)$ irreducible representation. First as we have done for the 1_1^- state at $E_r=0.1$ MeV, we introduce the attractive three-body force of Eq. (9), with the same parameters as the case of the 1_1^- state, i.e., $\mu=0.1$ fm^{-2} and $V_0=-110$ MeV. With this three-body force, the 1^- state gains more binding energy and becomes a much sharper resonance, with $E_r=2.8$ MeV and $\Gamma=0.5$ MeV, which we denote the 1_{II}^- state. We then calculate the squared overlap with the states $|(5,0)_1\rangle$ and $|(3,1)_1\rangle$ defined in Eq. (13), corresponding to the genuine state and ^{9}Be analog in the SU(3) model interpretation, respectively. We obtain complex values $0.01+0.001i$ and $0.39+0.02i$ for the $(5,0)_1$ and $(3,1)_1$ states, respectively. Here, in this case, the squared overlap is defined by $\langle\widetilde{1_{II}^-}|(\lambda,\mu)_1\rangle\langle(\lambda,\mu)_1|1_{II}^-\rangle$, where the complex conjugate is not taken in the bra state. For both values, the imaginary parts are much smaller than the real parts, due to the narrower width of the state, so that we can safely discuss the physical quantity as usual, by taking only the real parts (see Table II). The real part of the squared overlap with $(3,1)_1$, 0.39, is much larger than the one with $(5,0)_1$, 0.01, indicating that this state much more resembles the $(3,1)_1$ state than the $(5,0)_1$ state, unlike the case of the 1_I^- state discussed above. This value 0.39 is similar to 0.45, the value of squared overlap between the 1_1^-

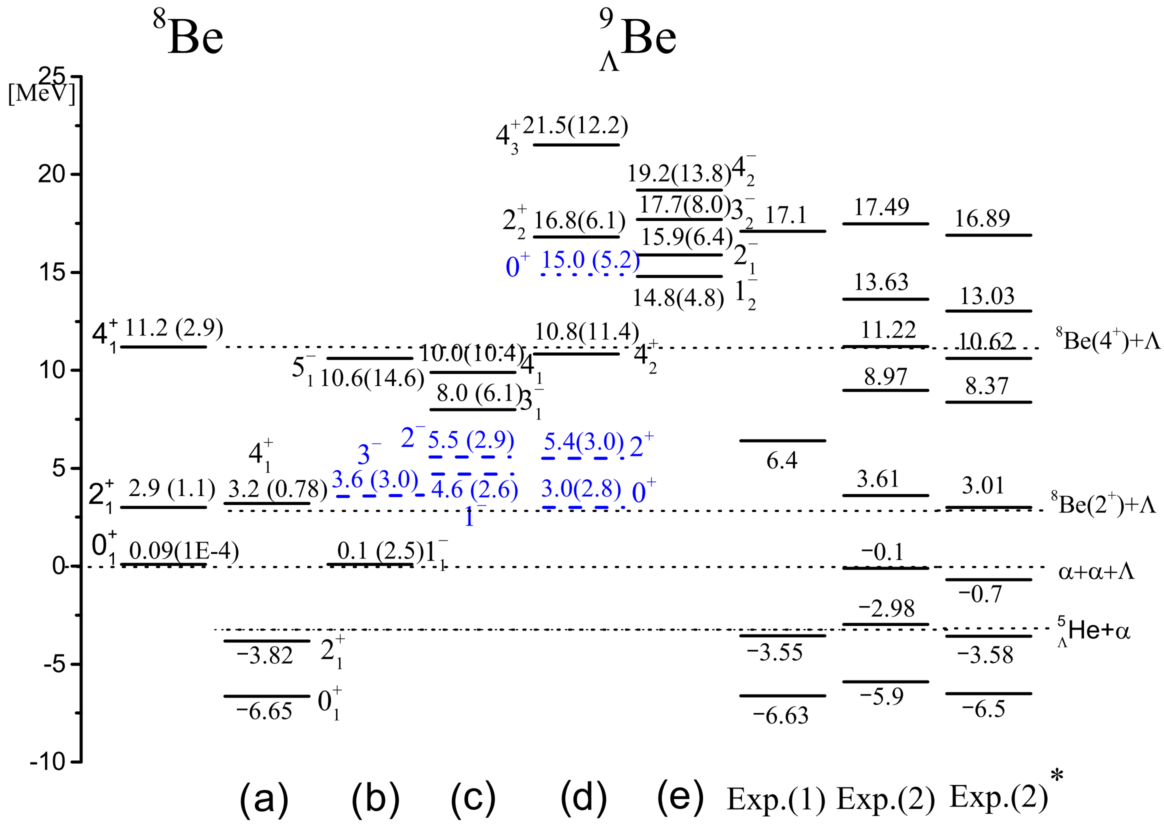

FIG. 5. Calculated energy spectra of ^{8}Be and $^{9}_{\Lambda}$Be with respect to $\alpha + \alpha + \Lambda$ three-body threshold. The values in parenthesis are decay widths. The spectra are categorized in a) ^{8}Be analog states, b) $^{9}_{\Lambda}$Be genuine states, c) ^{9}Be analog states, d) new states of positive parity, and e) new states of negative parity. The states colored in black are calculated in all three channels (C = 1–3) while the blue ones are calculated in only the $C = 1$ and $C = 2$ channels. The observed energies of $^{9}_{\Lambda}$Be in column Exp.(1) are taken from Refs. [34–36]. The observed energies of $^{9}_{\Lambda}$Be in column Exp.(2) are taken from Refs. [23,24]. And in column Exp.(2)*, we show the recalibration of the observed values in column Exp.(2) according to Ref. [40].

state obtained with the same three-body force and the $(3, 1)_1$ state in Eq. (13). Thus, we can conclude that this inherently "missing" 1^- state in our more precise calculations with the correct resonance boundary condition, is of the ^{9}Be analog nature and corresponds to the 1^-_2 state in column c′) of Fig. 3.

The overlaps between the calculated 1^- states and SU(3)-like configurations give clear structures of the two 1^- states. On the other hand, it is also interesting to give the amount of ^{8}Be$(0^+) + \Lambda$ and ^{8}Be$(2^+) + \Lambda$ components in these two 1^- states, where ^{8}Be(0^+) and ^{8}Be(2^+) are calculated within the present model space. Accordingly, we calculate the spectroscopic S^2 factor of the ^{8}Be $+\Lambda$ channel for these two artificial 1^- states (1^-_I and 1^-_{II}):

$$\mathscr{S} = \int \mathscr{Y}(R)^2 R^2 dR, \tag{15}$$

where $\mathscr{Y}(R)$, the reduced width amplitudes (RWAs), are defined by

$$\mathscr{Y}(R) = \sqrt{\frac{2!}{2!1!}} \left\langle 1^-_I(1^-_{II}) \middle| \left[\frac{\delta(R_3' - R)}{R_3'^2} Y_1(\hat{R}_3{}'), \varphi_i(^{8}\mathrm{Be}) \right]_{J=1} \right\rangle. \tag{16}$$

In the above equation, $\varphi_i(^{8}$Be$)$ is the wave function of the ^{8}Be(0^+) state or the ^{8}Be(2^+) state and R_3' is the relative coordinate between ^{8}Be and Λ. For the 1^-_I state, the S^2-factor values are 0.45 for the ^{8}Be$(0^+) + \Lambda$ channel and 0.30 for the ^{8}Be$(2^+) + \Lambda$ channel. And for the 1^-_{II} state, it gives 0.30 for the ^{8}Be$(0^+) + \Lambda$ channel and 0.40 for the ^{8}Be$(2^+) + \Lambda$ channel. Then, totally the p-wave Λ has large percentages in these two 1^- states, which are 0.75 and 0.7, respectively, for the 1^-_I state and the 1^-_{II} state.

Despite the fact that the p-wave Λ has large percentages in these two 1^- states, the s-wave Λ component might not be negligible. We then calculate the α spectroscopic S^2 factor with the reduced amplitude $\mathscr{Y}$ defined as

$$\mathscr{Y}(R) = \sqrt{\frac{2!}{1!1!}} \left\langle 1^-_I(1^-_{II}) \middle| \left[\frac{\delta(R_1' - R)}{R_1'^2} Y_1(\hat{R}_1{}'), \phi(^{5}_{\Lambda}\mathrm{He}) \right]_{J=1} \right\rangle, \tag{17}$$

where $\phi(^{5}_{\Lambda}$He$)$ is the wave function of the $^{5}_{\Lambda}$He(0^+) state and R_1' is the relative coordinate between $^{5}_{\Lambda}$He and α. This gives S^2-factor values of about 0.2 and 0.07 for the 1^-_I state and the 1^-_{II} state, respectively, which are much smaller than the ones with ^{8}Be $+\Lambda$ channels.

These 3^-, 1^-, and 2^- states are additionally shown in Fig. 5, denoted in blue. Since it is difficult to analyze the resonant wave functions with broad widths, such as the 3_1^-, 4_1^-, and 5_1^- states, due to ill behavior of their asymptotic behaviors, we just tentatively assign these states in column b) and c), i.e., the 5_1^- state in b) and 3_1^- and 4_1^- states in c). This assignment, however, seems to be reasonable since now we find the "missing" 3^-, 1^-, and 2^- states below the 3_1^-, 4_1^-, and 5_1^- states, which can compensate the missing spectra, to be consistent with the $J^\pi = 1^-,\ 3^-,\ 5^-$ given by $(\lambda, \mu) = (5, 0)$ and $J^\pi = 1^-,\ 2^-,\ 3^-,\ 4^-$ given by (3,1) SU(3) irreducible representations.

We should mention a possible reason why the states that are "missing" in our calculations survive as resonances in Ref. [2]. In the former cluster model calculations, all these states have a Λ particle in a dominantly p state with respect to the ^{8}Be(2^+) core, so that they can survive as resonances, since they can be trapped inside their centrifugal barriers. On the other hand, in our present calculations, the $^8\text{Be}(0^+) + \Lambda$ component might be more mixed to make the widths of the states broader, due to larger decay energies. The fact that the calculation with the restricted rearrangement channels ($C = 1$ and $C = 2$ only) gives clear poles for the "missing" states, however, indicates that their survivals as resonances are very sensitive to their structures.

C. New states of $^9_\Lambda$Be

Besides the states displayed in column a)–c) of Fig. 3, whose structures are studied by many authors, we newly find another three positive parity states, 2_2^+, 4_2^+, and 4_3^+ states, and four negative parity states, 1_2^-, 2_1^-, 3_2^-, and 4_2^- states, which are shown separately in columns d) and e) of Fig. 5. They are located at more than 10 MeV above the $\alpha + \alpha + \Lambda$ threshold, with non-negligible widths as resonances, and have never been pointed out by the other authors before. We should note that these states could never be found without imposing a correct boundary condition of resonances, like the CSM in the present treatment of resonances.

As was mentioned in the previous subsection, these states also have broad widths and it is difficult to practically deal with the resonant wave functions. However, as was done in the previous subsection, for further information about the group of the new states, we solve the three-body problem with a practically restricted model space, with only $C = 1$ and $C = 2$ rearrangement channels, and search for further complex energy poles by the CSM. Then another three resonances show up, two 0^+ and one 2^+ states, at 3.0 MeV with $\Gamma = 2.8$ MeV, 5.4 MeV with $\Gamma = 3.0$ MeV, and 15.0 MeV with $\Gamma = 5.2$ MeV, respectively. They are shown in column d) of Fig. 5 denoted by blue. The reason why the additional resonances appear when solved in the practically restricted model space may be similar to that of the case of the negative parity states discussed in the previous subsection. The inclusion of the channel $C = 3$ may increase the $^8\text{Be} + \Lambda$ channel components, and eventually its continuum-like components as well, to make the states difficult to survive as resonances with a $^8\text{Be} + \Lambda$-like structure. Thus, together with the artificial three states, as shown in column d) of Fig. 5, two groups of the 0^+, 2^+, and 4^+ states may exist and each group seems to form a rotational band, possibly of $^8\text{Be} + \Lambda$ structure.

TABLE IV. Energy spectra of $^9_\Lambda$Be with respect to the α-α-Λ threshold. We present our calculated energy together with the decay width for resonant states. The KEK(E336) are the experimental data obtained in 1998 by KEK [23,24]. The last column marked as KEK(E336)* are the recalibration of the KEK(E336) (π^+, K^+) values according to Ref. [40]. All energies are given in MeV.

	Present work		KEK(E336)	KEK(E336)*
$^9_\Lambda$Be	E_r	Γ	E_r^{exp}	$E_r^{\text{exp*}}$
0_1^+	−6.65	–	-5.90 ± 0.07	-6.50 ± 0.07
2_1^+	−3.82	–	-2.97 ± 0.07	-3.57 ± 0.07
1_1^-	0.1	2.5	-0.10 ± 0.13	-0.70 ± 0.13
3_1^-	8.0	6.1	3.61 ± 0.13	3.01 ± 0.13

Finally, in Table IV, we compare our results with the observed data obtained by KEK with the (π^+, K^+) reaction in 1998 [23,24]. First, the observed binding energy of KEK(E336) is $B_\Lambda = 5.99 \pm 0.07$ MeV, which is quite different from our results even if we include the systematic error, ± 0.36 MeV [23]. It should be noted that this observed value is calibrated by the emulsion data of $^{12}_\Lambda$C. In Ref. [40], Gal *et al.* suggested to add this B_Λ by 0.6 MeV for recalibration. As a result, we have $B_\Lambda = 6.59 \pm 0.07$ MeV, which is also listed in the last column of Table IV. And for the first excited states, $E_{\text{ex}} = 2.93 \pm 0.07$ MeV, is similar to our results, $E_{\text{ex}} = 2.83$ MeV and another experimental data in Ref. [35], $E_{\text{ex}} = 3.079 \pm 0.07$ MeV.

Second, for the resonances, our calculated $^9_\Lambda$Be genuine state, 1_1^- state is consistent with the third experimental state. The fifth observed data, 8.97 MeV, is close to our 3_1^-, ^{9}Be analog state. In addition, the observed sixth state, 11.2 MeV, is close to our 4_2^+ state, and the seventh state, 13.63 MeV, corresponds to 1_2^-. And the eighth observed data, 17.49 MeV, is close to our 2_1^- state or 3_2^- state.

Especially, the fourth experimental value, 3.61 MeV, is considered to be the 3^- state, according to Ref.[4]. The 6.4 MeV state in column Exp. (1) of Fig. 5, is considered to be the 1^- state, due to the enhancement of recoilless transition ($\Delta L = 0$) in the $^9\text{Be}(K^-, \pi^-)^9_\Lambda\text{Be}$ reaction. We cannot find these two states in our calculation within a rotated angle $\theta \sim 26$ degrees. However, it should be noted that we do not perform any (π^+, K^+) or (K^-, π^-) reaction calculations in the present work. To compare our results with the experimental data, it is necessary to calculate the reaction cross section, which is in our future work.

IV. SUMMARY

We have calculated energy spectra of $^9_\Lambda$Be within the framework of the $\alpha + \alpha + \Lambda$ three-body model. In this work, we employed the α-α interaction which reproduces the observed $\alpha\alpha$ scattering data. The Pauli forbidden states $(0s, 1s, 0d)$ between two αs are ruled out by orthogonality condition model (OCM). We employed the $\alpha\Lambda$ potential by a folding procedure of *YNG-NF* ΛN with an α wave function.

Here, we adjust even and odd states of the ΛN interaction so as to reproduce the observed binding energies of ground states in ${}^{5}_{\Lambda}$He and ${}^{9}_{\Lambda}$Be. For the resonant states of ${}^{9}_{\Lambda}$Be, we employed the CSM which is one of the powerful methods to obtain the energy pole and decay width.

As a result, we categorize the level structure obtained here into (a) to (e) which are shown in Fig. 5: (a) is ^{8}Be-analog states, (b) is ${}^{9}_{\Lambda}$Be genuine states, (c) is ^{9}Be analog states, which are pointed out by Bandō and Motoba *et al.* [1–3], and (d) and (e) are new states which have never been pointed out by Bandō and Motoba *et al.* [1–3]. The points emphasized here are as follows:

(1) The calculated binding energy of the 2^+_1 state is -3.82 MeV, which does not contradict the corresponding data, -3.55 MeV. The calculated 4^+_1 state is a resonant state at 3.2 MeV with $\Gamma = 0.78$ MeV. Here, note that Motoba *et al.* [2] obtain a resonant energy only within the bound state approximation. Our calculated energies of ^{8}Be analog states, $0^+, 2^+, 4^+$ states are the same as those by Motoba *et al.* [2]. To confirm these three states are ^{8}Be analog states, we calculate s-wave components of the Λ particle coupling to the ^{8}Be core and find the component to be 96%, 95%, and 93%, which are similar values by Motoba *et al.* [2].

(2) The calculated first 1^- state is obtained by 0.1 MeV above the $\alpha + \alpha + \Lambda$ three-body model with $\Gamma = 2.5$ MeV. To analyze the wave function of the 1^- state, we introduce a three-body force to make this state artificially bound, and then calculate the squared overlap of the artificial bound state wave function and relative wave function by $(\lambda, \mu) = (5, 0)$ and (3,1) SU(3) representation. We find the squared overlap value for the (5,0) representation is 45% and for the (3,1) representation 1%. Then, we confirm the 1^-_1 is the ${}^{9}_{\Lambda}$Be genuine state.

(3) As shown in b) and c) of Fig. 5, the 3^-, 1^-, and 2^- states are missing which are different from those by Motoba *et al.* [2]. To analyze it, we solve the three-body problem of ${}^{9}_{\Lambda}$Be with a restricted model space, that is, with only $C = 1$ and $C = 2$ channels in Fig. 1 and we find resonance states. From the fact that the inclusion of the $C = 3$ channel causes the disappearance of the resonant state, we find that due to the large overlap of the ^{8}Be $+\Lambda$ structure, the three resonant states are melted into continuum states. Also, by analyzing the wave function of the 'missing' 1^- state, we confirm that the states of c) of Fig. 5 are categorized into the '^{9}Be analog' states, which was pointed out by Bandō and Motoba *et al.* [1–3].

(4) We obtain new states of positive parities and negative parities, which have never been pointed out by Bandō and Motoba *et al.* [1–3], as shown in d) and e) of Fig. 5. These states are located at around 10 MeV to 20 MeV above the $\alpha + \alpha + \Lambda$ three-body threshold with larger decay widths.

(5) Finally, we compare our results with the observed data obtained so far. It is striking that our binding energy of the 1^- state, ${}^{9}_{\Lambda}$Be genuine state, is consistent with the observed energy, -0.1 MeV, The observed data of $E = 8.97$ MeV is close to 8.0 MeV calculated for the 3^- state. Our 5^-_1, 4^-_1, or 4^+_2 states may correspond to the observed $E = 11.22$ MeV state. The observed $E = 13.67$ MeV state is close to the 1^-_2 state and the observed $E = 17.49$ MeV state is close to our 2^+_2 and 3^-_2 states. At the peak, about 17.1 MeV [Exp.(1)], Yamada *et al.* [4] pointed out that the state at this energy should be an 's-hole' substitutional state within the framework of $\alpha + 3N + N + \Lambda$ cluster model, which was not included in our present work. To confirm the observed states theoretically, it is necessary to calculate the (π^+, K^+) reaction cross section. This is our future work.

ACKNOWLEDGMENTS

This work is supported by the RIKEN-MOST collaboration and Grants-in-Aid for Scientific Research on Innovative Areas (Nos. JP18H05407, JP18H05236, and JP18K03658) and JSPS Grant-in-Aid for Scientific Research (Nos. JP16H03995 and JP18K03658). One of the authors (Q.W.) is supported by the National Natural Science Foundation of China (12075117, 11535005, 11690030) and National Major state Basic Research and Development of China (2016YFE0129300).

[1] T. Motoba, H. Bandō, and K. Ikeda, Prog. Theor. Phys. **70**, 189 (1983).
[2] T. Motoba, H. Bandō, K. Ikeda, and T. Yamada, Prog. Theor. Phys. Suppl. **81**, 42 (1985).
[3] H. Bandō, K. Ikeda, and T. Motoba, Prog. Theor. Phys. **69**, 918 (1983).
[4] T. Yamada, K. Ikeda, H. Bandō, and T. Motoba, Phys. Rev. C **38**, 854 (1988).
[5] Y. Zhang, E. Hiyama, and Y. Yamamoto, Nucl. Phys. A **881**, 288 (2012).
[6] E. Hiyama, M. Kamimura, T. Motoba, T. Yamada, and Y. Yamamoto, Phys. Rev. C **53**, 2075 (1996).
[7] E. Hiyama, Y. Yamamoto, T. Motoba, and M. Kamimura, Phys. Rev. C **80**, 054321 (2009).
[8] S. N. Nakamura *et al.*, Phys. Rev. Lett. **110**, 012502 (2013).
[9] E. Hiyama, M. Kamimura, K. Miyazaki, and T. Motoba, Phys. Rev. C **59**, 2351 (1999).
[10] B. N. Lu, E. Hiyama, H. Sagawa, and S. G. Zhou, Phys. Rev. C **89**, 044307 (2014).
[11] M. Isaka, K. Fukukawa, M. Kimura, E. Hiyama, H. Sagawa, and Y. Yamamoto, Phys. Rev. C **89**, 024310 (2014).
[12] Y. Funaki, M. Isaka, E. Hiyama, T. Yamada, and K. Ikeda, Phys. Lett. B **773**, 336 (2017).
[13] K. Tanida *et al.*, Phys. Rev. Lett. **86**, 1982 (2001).
[14] R. H. Dalitz and A. Gal, Phys. Rev. Lett. **36**, 362 (1976).
[15] R. H. Dalitz and A. Gal, Ann. Phys. **131**, 314 (1981).
[16] C. W. Johnson *et al.*, arXiv:1912.00451.
[17] J. Aguilar and J. M. Combes, Commun. Math. Phys. **22**, 269 (1971).
[18] E. Balslev and J. M. Combes, Commun. Math. Phys. **22**, 280 (1971).
[19] B. Simon, Commun. Math. Phys. **27**, 1 (1972).

[20] Y. K. Ho, Phys. Rep. **99**, 1 (1983).
[21] N. Moiseyev, Phys. Rep. **302**, 212 (1998).
[22] J. Lee, Q. Wu, Y. Funaki, H. Zong, and E. Hiyama, Few Body Syst. **60**, 30 (2019).
[23] O. Hashimoto and H. Tamura, Prog. Part. Nucl. Phys. **57**, 564 (2006).
[24] S. Ajimura, K. Aoki, H. Bhang *et al.*, Nucl. Phys. A **639**, 93c (1998).
[25] E. Hiyama, Y. Kino, and M. Kamimura, Prog. Part. Nucl. Phys. **51**, 223 (2003).
[26] E. Hiyama, M. Kamimura, T. Motoba, T. Yamada, and Y. Yamamoto, Prog. Theor. Phys. **97**, 881 (1997).
[27] H. Akikawa, S. Ajimura, R. E. Chrien *et al.*, Phys. Rev. Lett. **88**, 082501 (2002).
[28] H. Tamura *et al.*, Nucl. Phys. A **752**, 155 (2005).
[29] Y. Yamamoto, T. Motoba, H. Himeno *et al.*, Prog. Theor. Phys. Suppl. **117**, 361 (1994).
[30] S. Aoyama, T. Myo, K. Kato, and K. Ikeda, Prog. Theor. Phys. **116**, 1 (2006).
[31] T. Myo, Y. Kikuchi, H. Masui, and K. Kato, Prog. Part. Nucl. Phys. **79**, 1 (2014).
[32] E. Hiyama, M. Isaka, M. Kamimura, T. Myo, and T. Motoba, Phys. Rev. C **91**, 054316 (2015).
[33] E. Hiyama, R. Lazauskas, J. Carbonell, and M. Kamimura, Phys. Rev. C **93**, 044004 (2016).
[34] R. Bertini *et al.*, Nucl. Phys. **368**, 365 (1981).
[35] M. May *et al.*, Phys. Rev. Lett. **51**, 2085 (1983).
[36] W. Bruckner *et al.*, Phys. Lett. B **62**, 481 (1976).
[37] B. F. Bayman and A. Bohr, Nucl. Phys. **9**, 596 (1958).
[38] J. P. Draayer and Y. Akiyama, J. Math. Phys. **14**, 1904 (1973)
[39] Y. Akiyama and J. P. Draayer, Comput. Phys. Commun. **5**, 405 (1973)
[40] A. Gal, E. V. Hungerford, and D. J. Millener, Rev. Mod. Phys. **88**, 035004 (2016)